Nonlinear thermo-mechanical buckling of axially compressive Ceramic-FGM-Metal cylindrical shell reinforced by orthogonal and spiral stiffeners

■ **MSc. LUU NGOC QUANG**
University of Transport technology

ABSTRACT: In this paper, the nonlinear buckling and postbuckling behavior of orthogonal and spiral stiffened Ceramic-FGM-Metal thin circular cylindrical shells under axial compression loads is presented. The material properties of shell and stiffeners are assumed to be continuously varied in the thickness direction respecting to the piecewise functions. The shells are reinforced by rings, stringers and spiral stiffeners attached to inside surface of shells. The thermal effects are also included and the material properties of Ceramic-FGM-Metal are assumed to be temperature-dependent. By using the Donnell shell theory and Galerkin method, the explicit forms of critical buckling load and expression of postbuckling load-deflection curves relation are obtained. The effects of the stiffeners, temperature change, volume fraction index of shells and stiffeners are numerically investigated.

KEYWORDS: Nonlinear thermo-mechanical buckling, functionally graded material (FGM), cylindrical shell, stiffener.

1. INTRODUCTION

Functionally graded material (FGM) is the advanced composite material made from a mixture of metal and ceramic. The buckling and postbuckling behavior of FGM stiffened cylindrical shells has been an interesting issue in recent years.

Najafizadeh et al. [1] studied the linearly mechanical stability of FGM cylindrical shells stiffened by FGM stiffeners subjected to axial compression loading. The shell properties are assumed to vary continuously through the thickness direction and the equilibrium and stability equations are derived using the Sander's assumption. Bich et al. [2], Dung and Nam [3] studied static and dynamic buckling behavior of FGM cylindrical shells with isotropic stiffeners by using Donnell shell theory and Galerkin method. Phuong et al [4,5] improved the smeared stiffener technique for spiral stiffeners to investigate the nonlinear postbuckling behavior of stiffened FGM and sandwich cylindrical shells under torsion load and axial compression.

According to the best knowledge of author, there is still no report in literature presented for nonlinear buckling behaviors of Ceramic-FGM-Metal cylindrical shells reinforced by spiral stiffener system subjected to axial compression load in thermal environment. Therefore, this paper presents an analytical approach on nonlinear axial compressive buckling of Ceramic-FGM-Metal cylindrical shells in the thermal environment reinforced by spiral and orthogonal FGM stiffeners.

2. CERAMIC-FGM-METAL CYLINDRICAL SHELL REINFORCED BY ORTHOGONAL AND SPIRAL STIFFENERS

Consider a Ceramic-FGM-Metal thin circular cylindrical shells with the coordinate system as shown in *Figure 2.1*. The Ceramic-FGM-Metal shell is reinforced by closely spaced the rings, stringers and spiral stiffeners attached to inside of the shell surface.

In case 1: the outside and inside layers of shell are full ceramic and metal, respectively. Whereas, FGM core layer varies from ceramic-rich interface $\left(z=-\frac{h}{2}+h_t\right)$ to metal-rich interface $\left(z=\frac{h}{2}-h_b\right)$ (as shown in *Figure 2.2a*).

In case 2: the outside and inside layers of shell are full ceramic and metal, respectively. Whereas, FGM core layer varies from metal-rich interface $\left(z=-\frac{h}{2}+h_t\right)$ to ceramic-rich interface $\left(z=\frac{h}{2}-h_b\right)$ (as shown in *Figure 2.2b*).

Effective properties of shell are given by:

- In case 1 (as illustrated in *Figure 2.2a*)

$$\left[E_{sh}(z),\alpha_{sh}(z)\right]=\begin{cases}\left[E_c,\alpha_c\right] & for\ -\frac{h}{2}\le z\le -\frac{h}{2}+h_t,\\ \left[E_c,\alpha_c\right]+\left[E_{mc},\alpha_{mc}\right]\left(\frac{z+h-2h_t}{2h_c}\right)^k & for\ -\frac{h}{2}+h_t\le z\le \frac{h}{2}-h_b,\\ \left[E_m,\alpha_m\right] & for\ \frac{h}{2}-h_b\le z\le \frac{h}{2}.\end{cases} \quad (1)$$

- In case 2 (as illustrated in *Figure 2.2b*)

$$\left[E_{sh}(z),\alpha_{sh}(z)\right]=\begin{cases}\left[E_m,\alpha_m\right] & for\ -\frac{h}{2}\le z\le -\frac{h}{2}+h_t,\\ \left[E_m,\alpha_m\right]+\left[E_{cm},\alpha_{cm}\right]\left(\frac{z+h-2h_t}{2h_c}\right)^k & for\ -\frac{h}{2}+h_t\le z\le \frac{h}{2}-h_b,\\ \left[E_c,\alpha_c\right] & for\ \frac{h}{2}-h_b\le z\le \frac{h}{2}.\end{cases} \quad (2)$$

Where: $E_{mc}=E_m-E_c; E_{cm}=E_c-E_m; \alpha_{mc}=\alpha_m-\alpha_c; \alpha_{cm}=\alpha_c-\alpha_m.$

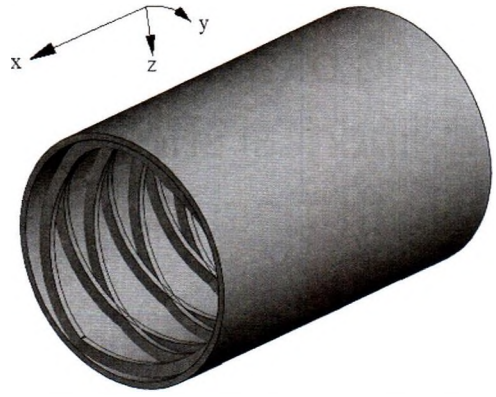

Figure 2.1: Geometry and coordinate system of a stiffened Ceramic-FGM-Metal circular cylindrical shell

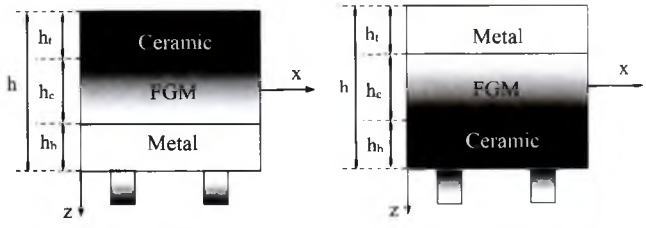

a) - Case 1 *b) - Case 2*

Figure 2.2: The material distribution in the shell and in the stiffeners for two models of Ceramic-FGM-Metal shell

In order to ensure the continuity between the shell and stiffeners, the effective properties of stiffeners are given by:

- In case 1 (as illustrated in *Figure 2.2a*)

$$[E_s,\alpha_s]=[E_m,\alpha_m]+[E_{cm},\alpha_{cm}]\left(\frac{2z-h}{2h_s}\right)^{k_s},\ h/2\le z\le h/2+h_s,$$

$$[E_r,\alpha_r]=[E_m,\alpha_m]+[E_{cm},\alpha_{cm}]\left(\frac{2z-h}{2h_s}\right)^{k_r},\ h/2\le z\le h/2+h_r, \quad (3)$$

$$[E_l,\alpha_l]=[E_m,\alpha_m]+[E_{cm},\alpha_{cm}]\left(\frac{2z-h}{2h_s}\right)^{k_l},\ h/2\le z\le h/2+h_l.$$

- In case 2 (as illustrated in *Figure 2.2b*)

$$[E_s,\alpha_s]=[E_c,\alpha_c]+[E_{mc},\alpha_{mc}]\left(\frac{2z-h}{2h_s}\right)^{k_s},\ h/2\le z\le h/2+h_s,$$

$$[E_r,\alpha_r]=[E_c,\alpha_c]+[E_{mc},\alpha_{mc}]\left(\frac{2z-h}{2h_s}\right)^{k_r},\ h/2\le z\le h/2+h_r, \quad (4)$$

$$[E_l,\alpha_l]=[E_c,\alpha_c]+[E_{mc},\alpha_{mc}]\left(\frac{2z-h}{2h_s}\right)^{k_l},\ h/2\le z\le h/2+h_l.$$

The subscripts c and m denote the ceramic and metal and sh, s, r, l denote the shell, stringer, ring and spiral, respectively.

3. THEORETICAL FORMULATION

The Donnell shell theory with von-Karman nonlinearity is used in this paper, the governing equations of problem including strain-displacement equations, stress-strain equations, forces and moment expressions, can be referred in Ref. [2-5]. The material distributed laws in Eqs. (1-4) are used to determine the stiffnesses of stiffened shells taking into account the improved smeared stiffener technique [4,5]. The equilibrium equations of Ceramic-FGM-Metal cylindrical shell taking into account the effects of elastic foundations, are presented as:

$$\begin{aligned}&\frac{\partial N_x}{\partial x}+\frac{\partial N_{xy}}{\partial y}=0,\ \frac{\partial N_{xy}}{\partial x}+\frac{\partial N_y}{\partial y}=0,\\&\frac{\partial^2 M_x}{\partial x^2}+2\frac{\partial^2 M_{xy}}{\partial x\partial y}+\frac{\partial^2 M_y}{\partial y^2}+\frac{N_y}{R}+N_x\frac{\partial^2 w}{\partial x^2}+2N_{xy}\frac{\partial^2 w}{\partial x\partial y}+N_y\frac{\partial^2 w}{\partial y^2}\\&+K_2\left(\frac{\partial^2 w}{\partial x^2}+\frac{\partial^2 w}{\partial y^2}\right)-K_1 w=0,\end{aligned} \quad (5)$$

Where: K_1 (N/m³) is the Winkler foundation modulus and K_2(N/m) is the shear stiffness of the Pasternak model.

Introducing a stress function φ(x,y), satisfied the conditions

$$N_x=\frac{\partial^2\varphi}{\partial y^2},\ N_y=\frac{\partial^2\varphi}{\partial x^2},\ N_{xy}=-\frac{\partial^2\varphi}{\partial x\partial y}. \quad (6)$$

The third equation of Eq. (5) can be rewritten by respecting to the unknown functions φ and w, as [4,5].

$$\begin{aligned}&C_{11}\frac{\partial^4 w}{\partial x^4}+C_{12}\frac{\partial^4 w}{\partial x^2\partial y^2}+C_{13}\frac{\partial^4 w}{\partial y^4}+C_{14}\frac{\partial^4\varphi}{\partial x^4}+C_{15}\frac{\partial^4\varphi}{\partial x^2y^2}+C_{16}\frac{\partial^4\varphi}{\partial y^4}\\&+\frac{1}{R}\frac{\partial^2\varphi}{\partial x^2}+\frac{\partial^2\varphi}{\partial y^2}\frac{\partial^2 w}{\partial x^2}+\frac{\partial^2\varphi}{\partial x^2}\frac{\partial^2 w}{\partial y^2}-2\frac{\partial^2\varphi}{\partial x\partial y}\frac{\partial^2 w}{\partial x\partial y}+K_2\left(\frac{\partial^2 w}{\partial x^2}+\frac{\partial^2 w}{\partial y^2}\right)-K_1 w=0,\end{aligned} \quad (7)$$

The compatibility equation can be written respected to the deflection and stress function by [4,5].

$$\begin{aligned}&D_{11}\frac{\partial^4\varphi}{\partial x^4}+D_{12}\frac{\partial^4\varphi}{\partial x^2\partial y^2}+D_{13}\frac{\partial^4\varphi}{\partial y^4}+D_{14}\frac{\partial^4 w}{\partial x^4}\\&+D_{15}\frac{\partial^4 w}{\partial x^2\partial y^2}+D_{16}\frac{\partial^4 w}{\partial y^4}-\left(\frac{\partial^2 w}{\partial x\partial y}\right)^2+\frac{\partial^2 w}{\partial x^2}\frac{\partial^2 w}{\partial y^2}+\frac{1}{R}\frac{\partial^2 w}{\partial x^2}=0,\end{aligned} \quad (8)$$

4. SOLUTION OF THE PROBLEM

Consider the Ceramic-FGM-Metal cylindrical shell with simply supported boundary conditions at the edges x = 0 and x = L. The solution forms of deflection and stress function can be chosen as

$$\begin{cases}w=w(x,y)=f_0+f_1\sin\left(\frac{m\pi}{L}x\right)\sin\left(\frac{n}{R}y\right)+f_2\sin^2\left(\frac{m\pi}{L}x\right),\\ \varphi=B_1\cos\left(2\frac{m\pi}{L}x\right)+B_2\cos\left(2\frac{n}{R}y\right)+B_3\sin\left(\frac{m\pi}{L}y\right)\sin\left(\frac{n}{R}y\right)\\ +B_4\sin\left(3\frac{m\pi}{L}x\right)\sin\left(\frac{n}{R}y\right)-\frac{1}{2}phy^2-\frac{1}{2}\sigma_{0y}hx^2.\end{cases} \quad (9)$$

Substituting the deflection form into the compatibility equation (8), the stress function parameters can be determined. Introducing w and φ into the Eq. (7). Then, applying the Galerkin method, we have:

$$-\frac{2\sigma_{0y}h}{R}-K_1(\beta_2+2\beta_0)=0, \quad (10)$$

$$\beta_1^2=\frac{ph}{X_{03}}\left(\frac{m\pi}{L}\right)^2+\frac{\sigma_{0y}h}{X_{03}}\left(\frac{n}{R}\right)^2-\left[\frac{X_{01}}{X_{03}}+\frac{X_{04}}{X_{03}}\lambda_2^2+\frac{X_{05}}{X_{03}}\lambda_2+\frac{K_2}{X_{03}}\left(\left(\frac{m\pi}{L}\right)^2+\left(\frac{n}{R}\right)^2\right)+\frac{K_1}{X_{03}}\right], \quad (11)$$

$$X_{06}\beta_2+8\left(\frac{m\pi}{L}\right)^2\beta_2 ph+X_{07}\beta_1^2+X_{08}\beta_1^2\beta_2-8\frac{\sigma_{0y}h}{R}-8K_2\left(\frac{m\pi}{L}\right)^2\beta_2-6K_1\beta_2-8K_{10}\beta_0=0, \quad (12)$$

The Ceramic-FGM-Metal cylindrical shell must be satisfied the closed condition, as:

$$\int_0^{2\pi R}\int_0^{L} \upsilon_{,y} dxdy = \int_0^{2\pi R}\int_0^{L}\left(\varepsilon_y^0 + \frac{w}{R} - \frac{1}{2}w_{,y}^2\right)dxdy = 0, \quad (13)$$

leads to:

$$8G_{12}^* ph - 8G_{11}^*\sigma_{0y}h + \frac{4}{R}(2\beta_0 + \beta_2) - \left(\frac{n}{R}\right)^2\beta_1^2 + 8\left(G_{24}^*\phi_1 - G_{12}^*\phi_{1x}^T + G_{11}^*\phi_{1y}^T\right) = 0. \quad (14)$$

Solving Eqs. (10-12) and Eq. (14), the expression of axial compression is obtained, as

$$p = \frac{1}{\left\{X_{07}F_{11} + \left[8\left(\frac{m\pi}{L}\right)^2 + X_{08}F_{11}\right]\beta_2\right\}h}\left\{X_{07}F_{12} + \left[X_{06} + X_{07}F_{13} + X_{08}F_{12} - 8K_2\left(\frac{m\pi}{L}\right)^2 - 4K_1\right]\beta_2 + \left(X_{07}F_{14} + X_{08}F_{13}\right)\beta_2^2 + X_{08}F_{14}\beta_2^3 - 8RK_1F_0\left(\frac{n}{R}\right)^2\left[\frac{X_{07}}{X_{03}} + \frac{X_{08}}{X_{03}}\beta_2\right]\left\{\left(G_{24}^*\phi_1 - G_{12}^*\phi_{1x}^T + G_{11}^*\phi_{1y}^T\right)\right\}\right\}. \quad (15)$$

From Eq. (15), taking $\beta_2 \to 0$, the upper buckling compressive load can be obtained by:

$$p_{upper} = -\frac{1}{X_{03}F_{11}h}\left[X_{03}F_{12} - 8RK_1F_0\left(\frac{n}{R}\right)^2\left(G_{24}^*\phi_1 - G_{12}^*\phi_{1x}^T + G_{11}^*\phi_{1y}^T\right)\right]. \quad (16)$$

From Eq. (9), It can be seen that the maximum deflection of the shells is determined by:

$$W_{max} = \beta_0 + \beta_1 + \beta_2. \quad (17)$$

Eq. (17) can be rewritten by respecting to the β_2, as:

$$W_{max} = F_{01}ph + F_{02} + (F_{03} + 1)\beta_2 + F_{04}\beta_2^2 + 8F_0\left(G_{24}^*\phi_1 - G_{12}^*\phi_{1x}^T + G_{11}^*\phi_{1y}^T\right) + \left[F_{11}ph + F_{12} + F_{13}\beta_2 + F_{14}\beta_2^2 - \frac{8RK_1(n/R)^2F_0}{X_{03}}\left(G_{24}^*\phi_1 - G_{12}^*\phi_{1x}^T + G_{11}^*\phi_{1y}^T\right)\right]^{1/2}. \quad (18)$$

The postbuckling load-maximal deflection curves of the Ceramic-FGM-Metal shells reinforced by spiral and orthogonal stiffeners in thermal environment can be investigated by combining Eq. (15) and Eq. (18).

5. NUMERICAL RESULTS AND DISCUSSIONS

Table 5.1 presents the critical buckling loads of orthogonally stiffened, spirally stiffened and unstiffened shells for case 1 and case 2 with different h_c/h ratios. As can be observed, the critical buckling loads of stiffened shells are larger than those of unstiffened shells, respectively. The significant effects of spiral stiffened shells are also obtained. With the same material quantity, the effect of spiral stiffeners is greater than one of orthogonal stiffeners. The results also show that the effects of h_c/h ratio on the critical buckling load are significant. The critical buckling load increases when the h_c/h ratio increases in all investigated cases.

Table 5.1. Critical buckling loads of orthogonally stiffened, spirally stiffened and unstiffened shells for case 1 and case 2 with different h_c/h ratios ($h = 0.005$ m, $h_t = h_b = 0.001$ m, $R = 0.5$ m, $L = 1$ m, $h_s = h_r = h_l = 0.01$ m, $b_s = b_r = b_l = 0.0025$m, $\Delta T = 0$ K)

P_{upper} (Gpa)	h_c/h	Spiral	Orthogonal	Unstiffened
Case 1	0.4	2.1360(1,6,80,31.91)*	1.8746 (4,8)**	1.6038(8,1)
	0.5	2.4178(2,7,63,33.32)	2.0238 (4.8)	1.6094(9,5)
	0.6	2.7204(2,6,52 ,34.14)	2.2165 (5,8)	1.6151(11,4)
Case 2	0.4	2.3618 (1,6,79,33.04)	1,9300(4,8)	1.6038(8,1)
	0.5	2.5930(1,5,63,33.32)	2.1241(4.8)	1.6094(9,5)
	0.6	2,9461 (1,5,52,34.14)	2.3573(5,7)	1.6151(11,4)

* the buckling mode, number of stiffener and stiffener angle (m, n, n_l, θ).

** the buckling mode $(m; n)$.

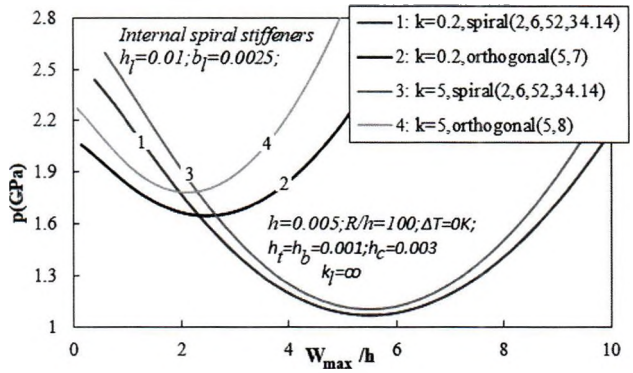

Figure 5.1: Effect of orthogonal and spiral stiffeners on the p - W_{max}/h postbuckling curves (Case 1)

Effects of orthogonal and spiral stiffeners on the p - W_{max}/h postbuckling curves of shells (case 1) are presented in *Figure 5.1*. Clearly, the postbuckling strength of spirally stiffened shells is larger than that of orthogonally stiffened shells with the small deflection. However, the opposite remarks are obtained for large deflection.

Effects of volume fraction index of FGM layer on the p - W_{max}/h postbuckling curves for the cases 1, are presented in *Figure 5.2*. The obtained results show that the postbuckling strength of shells increases when the volume fraction index increases. It seems that, unlike the upper buckling load, the differences between lower critical buckling loads for three investigated cases are insignificant.

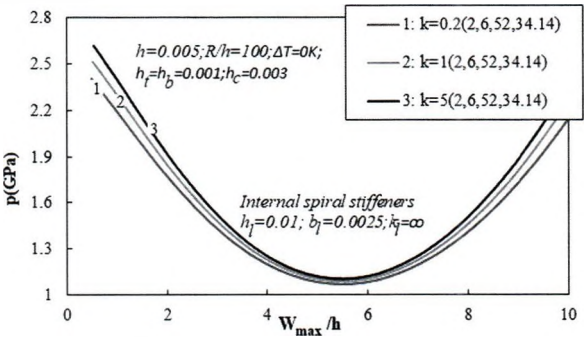

Figure 5.2: Effects of volume fraction index of FGM layer on the p - W_{max}/h postbuckling curves (Case 1)

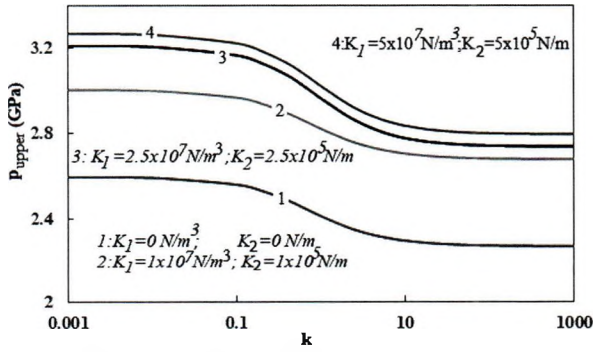

Figure 5.3: Effects of foundation parameters on the P_{upper} - k curves (Case 2)

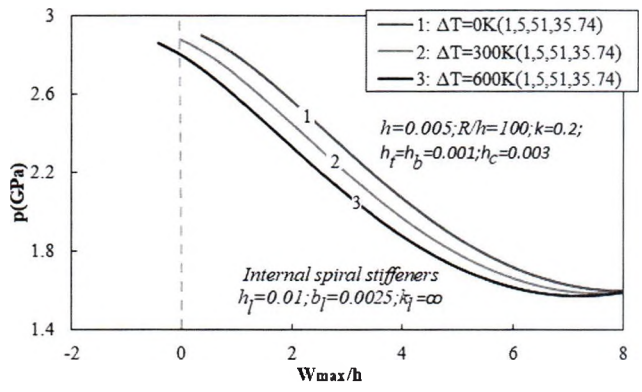

Figure 5.4: Effects of thermal temperature on the p - W_{max}/h postbuckling curves (Case 2)

Effects of foundation parameters on the P_{upper} - k curves of shells can be recognized in *Figure 5.3* (Case 2). Clearly, the significant effects of foundation stiffnesses can be obtained and the large effects are recognized with the small values of volume fraction index of FGM.

Effects of thermal temperature on the p - W_{max}/h postbuckling curves are shown in *Figure 5.4*. The results show that the critical buckling load and the postbuckling strength of shells significantly decreases when the thermal temperature increases. Additionally, the thermal pre-deflection can be clearly recognized in the investigated cases.

6. CONCLUSIONS

In this paper, an analytical approach is presented to analyze the nonlinear buckling and post-buckling behavior of Ceramic-FGM-Metal cylindrical shell under an axial compression, surrounded by elastic foundation and in a thermal environment. Two cases of distributed laws of Ceramic-FGM-Metal cylindrical shell are analyzed. The obtained results show the significant remarks, as follow:

- The explicit expressions for critical buckling loads and nonlinear postbuckling curves are obtained and the thermal terms in shell and spiral stiffeners are taken into account.
- The critical compression load of spiral stiffened shell is greater than the one of orthogonal stiffened shell.
- The uniformly distributed temperature, stiffeners, FGM core layer, foundation, and volume fraction index significantly affect to the buckling and post-buckling behavior of the shell.

References

[1]. Najafizadeh M., Hasani A, Khazaeinejad P. (2008), *Mechanical stability of functionally graded stiffened cylindrical shells*, Applied Mathematical Modelling 33, 1151-1157.

[2]. Bich DH, Dung DV, Nam VH, Phuong NT. (2013), *Nonlinear static and dynamic buckling analysis of imperfect eccentrically stiffened functionally graded circular cylindrical thin shells under axial compression*, International Journal of Mechanical Sciences 74, 190-200.

[3]. Dung DV, Nam VH. (2014), *Nonlinear dynamic analysis of eccentrically stiffened functionally graded circular cylindrical thin shells under external pressure and surrounded by an elastic medium*, European Journal of Mechanics - A/Solids, 46, 42-53.

[4]. Phuong NT, Luan DT, Nam VH, Hieu PT. (2019), *Nonlinear approach on torsional buckling and postbuckling of functionally graded cylindrical shells reinforced by orthogonal and spiral stiffeners in thermal environment*, Proceedings of the Institution of Mechanical Engineers, Part C: Journal of Mechanical Engineering Science 233(6), 2091-2106.

[5]. Phuong NT, Nam VH, Trung NT, Duc VM, Phong PV. (2019), *Nonlinear Stability of Sandwich Functionally Graded Cylindrical Shells with Stiffeners Under Axial Compression in Thermal Environment*, International Journal of Structural Stability and Dynamics 19(07), 1950073.

Data of issue: 16/6/2021
Data of posted: 17/7/2021
Reviewers: Prof. Dr. Vu Hoai Nam
Prof. Dr. Nguyen Thi Phuong